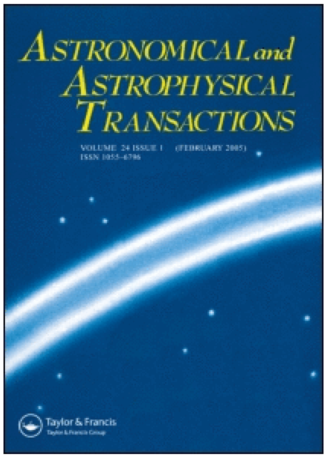

Astronomical & Astrophysical Transactions
The Journal of the Eurasian Astronomical Society
Publication details, including instructions for authors and subscription information:
http://www.informaworld.com/smpp/title~content=t713453505

Generation of MHD turbulence by non-equilibrium ion velocity distributions in the outer heliosphere and the interstellar medium: magnetohydro-thermodynamic and kinetic views

H. J. Fahr [a]; I. V. Chashei [b]
[a] Department of Astrophysics, Argelander Institute for Astronomy, University of Bonn, Bonn, Germany
[b] Lebedev Physical Institute, Moscow, Russia

Online Publication Date: 01 December 2007
To cite this Article: Fahr, H. J. and Chashei, I. V. (2007) 'Generation of MHD turbulence by non-equilibrium ion velocity distributions in the outer heliosphere and the interstellar medium: magnetohydro-thermodynamic and kinetic views', Astronomical & Astrophysical Transactions, 26:6, 621 - 636
To link to this article: DOI: 10.1080/10556790701610316
URL: http://dx.doi.org/10.1080/10556790701610316

Astronomical and Astrophysical Transactions
Vol. 26, No. 6, December 2007, 621–636

Taylor & Francis
Taylor & Francis Group

Generation of MHD turbulence by non-equilibrium ion velocity distributions in the outer heliosphere and the interstellar medium: magnetohydro-thermodynamic and kinetic views

H. J. FAHR*† and I. V. CHASHEI‡

†Department of Astrophysics, Argelander Institute for Astronomy, University of Bonn, Auf dem Huegel 71, 53121 Bonn, Germany
‡Lebedev Physical Institute, Moscow, Russia

(Received 19 July 2007)

We show that energetic ions, appearing in plasmas due to injection of charge-exchange-induced new ions into the magnetized plasma background, flow due to their freely convertible energy drive turbulences of Alfvenic and magneto-acoustic types. This becomes important especially under conditions of strongly charge-exchanging fluids with supersonic differential bulk velocities, as is the condition in the inner heliosphere. These ion-driven waves lead to strongly enhanced fluctuation amplitudes. As a consequence, both low- and high-energy ion populations can partly reabsorb these wave energies, and thereby experience non-thermal heatings. As a quantitative example, we calculate the non-adiabatic behaviours of solar wind ions and pick-up ions expanding with the solar wind towards large solar distances. While pick-up ions behave nearly isothermal, normal solar wind ions behave pseudo-polytropically with negative effective polytropic indices that describe temperature increases at diverging plasma flows. Furthermore, we demonstrate that charge-exchanging plasmas in the inner and outer heliosheath, such as the solar wind and the interstellar ion and atom fluids, lead to unexpectedly enhanced turbulence amplitudes of low frequency Alfven and magneto-acoustic waves. Connected with that, lower periods for the relaxation of non-equilibrium ion distribution functions and lower coefficients for the spatial diffusion of galactic cosmic rays must be expected in the heliosheath. Finally, we study the interstellar turbulence generation caused by supernova shock fronts due to their generation of mirror-unstable anisotropic ion distribution functions downstream of the shock. We demonstrate that an unexpectedly high percentage of the shock-entropized thermal energy of the downstream ions is converted into magneto-acoustic turbulences. This not only characterizes the region immediately downstream of the SN shock as a high-turbulence region, but may, judged in a statistical view, also point to an increase of the average turbulence levels in the interstellar medium in general.

Keywords: Heliosphere; MHD turbulence; Plasma heating; Ion distribution function

1. Introduction

Interactions of interstellar particles and Magnetohydrodynamic (MHD) turbulence are of great relevance for the physics of the outer heliosphere including the heliosheath, *i.e.* the distant

*Corresponding author. Email: hfahr@astro.uni-bonn.de

Astronomical and Astrophysical Transactions
ISSN 1055-6796 print/ISSN 1476-3540 online © 2007 Taylor & Francis
http://www.tandf.co.uk/journals
DOI: 10.1080/10556790701610316

regions of the shocked solar wind. These interactions can be regarded as explanations of two important, obviously interrelated findings in heliospheric physics: one is the fact that the primary solar wind protons do not cool off adiabatically with distance as expected in earlier times, but appear to be heated [1, 2]. The other one is that secondary protons, embedded in the solar wind as pick-up ions, behave quasi-isothermal at their motion to the outer heliosphere and appear to represent conformally invariant power law spectra [3, 4]. These two eminent phenomena must be physically closely connected with each other, which we are going to investigate more deeply in this paper.

In the first part of this paper, we consider the heating of the distant solar wind by dissipative processes associated with resonant energy absorption both from background turbulence convected with the solar wind and high frequency MHD waves generated locally by freshly injected pick-up ions [5–7].

As is presently expected, the partially ionized local interstellar medium (LISM) before interacting with the heliospheric plasma on the upwind side most probably undergoes an outer bow shock and, after conversion into a submagnetosonic plasma flow, passes around the heliopause [8]. While the ionized interstellar component there undergoes abrupt changes of its dynamical properties, the neutral interstellar component first continues to flow downstream of the shock with its unperturbed LISM properties. As a consequence of this abrupt disequilibration, the two fluids immediately after the bow shock passage are out of dynamical and thermodynamical equilibrium, *i.e.* neutral LISM atoms move with a higher bulk velocity and are cooler than the LISM ions. Due to intensive local charge-exchange couplings between neutral atoms and protons, these disjunctive properties tend to adapt to each other via momentum and energy exchanges. It turns out that the charge exchange period is shorter than the relaxation period. Hence, the distribution functions cannot relaxate rapidly enough to their highest-entropy forms, *i.e.* shifted Maxwellians. The resulting deviations of proton and H-atom distribution functions in the outer interface region from associated fully relaxated functions, *i.e.* shifted Maxwellians, have recently been studied and quantitatively been calculated on the basis of a semi-kinetic two-fluid approach by Fahr and Bzowski [9, 10]. In their approach, however, only Coulomb collision processes were taken into account as relevant relaxation processes, and it was shown that under these auspices non-relaxated distributions develop in the interface, especially under conditions of low LISM ionization degrees, *i.e.* low LISM proton densities. Also in the inner heliosheath region where low proton densities and high proton temperatures prevail, Coulomb relaxation becomes very inefficient [10].

Considering quasilinear wave–particle interactions in the heliospheric interface, we thus looked more carefully into alternative relaxation processes that support the entropization of the perturbed low-entropy distribution functions [11]. A third problem considered below is the evolution of the velocity distribution functions of plasma constituents by the passage of plasma from the upstream to the downstream side of the solar wind termination shock. For that purpose, we have developed a specifically appropriate form of the Boltzmann equation describing the ion distribution function in the solar wind plasma bulk frame [12].

2. Injection of free ion energy into MHD power

When neutral atoms are ionized in the magnetized solar wind plasma, then newly born ions are very rapidly picked up into a gyration about co-convected magnetic $\vec{B}$-field lines frozen into the solar wind plasma flow due to the electromotoric Lorentz forces. At the same time, there is, however, no systematic force accelerating them along the magnetic field lines. As a result, freshly created ions form an initial torus configuration in the comoving Solar Wind (SW) velocity space, which is unstable to the generation of Alfven waves [13–15]. Secondary ions just after their injection undergo fast pitch-angle scattering from an initial torus configuration in SW velocity space onto a much more stable [15] bi-spherical hemispheric shell configuration. The two associated hemispheres correspond to velocities $\pm v_{\mathrm{A}}$ in the SW plasma bulk frame, where v_{A} denotes the Alfven speed of the ambient plasma. Local Alfven wave generation by pick-up ions was for the first time detected by Huddleston and Johnstone [16] in the plasma environment of comet Halley. The data on magnetic field fluctuation spectra measured by Giotto spacecraft during its flyby at comet Halley have shown a systematic increase in the power level of high-frequency magnetic field turbulence when the spacecraft was approaching the comet [16]. Enhanced magnetic fluctuation powers were observed in the wavenumber range $k \geq k_L$, where $k_L \approx \Omega_i / V_{\mathrm{w}}$, with Ω_i being the gyrofrequency of pick-up ions and V_{w} being the solar wind speed. The measured value of k_L corresponded to the local gyrofrequency of singly charged oxygen atoms.

This clearly eminent power generation mechanism was theoretically further studied as an additional energy source to heat the distant solar wind via waves driven by injected interstellar pick-up ions [5–7, 17, 18]. We estimate below the energy pumped from pick-up ions to MHD turbulence power in the distant solar wind. At heliospheric regions beyond 5 AU, the orientation of the magnetic field $\vec{B}$ with respect to the radial solar wind flow direction (especially in the ecliptic) becomes nearly orthogonal. Thus, the associated bi-spheres centred around the reference systems of upgoing and downgoing (*i.e.* with respect to $\vec{B}$) Alfven waves become symmetrically populated. Under these conditions, at the event of injection, the new secondaries have an ion velocity v, which in the solar wind frame is equal to the solar wind velocity V_{w}, with $V_{\mathrm{w}} \gg v_{\mathrm{A}}$. Consequently, after rapid pitch-angle scattering to the accessible bi-spheres (only a loss of energy is permitted for resonantly pitch-angle scattered ions!) within each of these fractional shells for upstream and downstream waves, one expects the following pick-up ion velocity v as judged in the SW frame:

$$v^2 = v_{\mathrm{A}}^2 + (V_{\mathrm{w}}^2 + v_{\mathrm{A}}^2) - 2 v_{\mathrm{A}} \sqrt{V_{\mathrm{w}}^2 + v_{\mathrm{A}}^2} \cos \vartheta, \tag{1}$$

where ϑ is the pitch angle of the resulting velocity v in the upstream wave frame. Since the newly generated secondary ions do quickly become randomly distributed on the accessible spherical shells, the distribution function for the populated velocities v is then simply given by the associated velocity space volume $\Delta v = v \cdot d \cos \vartheta(v)$, *i.e.* is given by the expression:

$$f(v) = \frac{-d \cos \vartheta(v)}{(1 - \cos \vartheta_{\max})}, \tag{2}$$

where the maximum possible pitch-angle $\vartheta_{\max}$ is simply given by:

$$\cos \vartheta_{\max} = \frac{v_{\mathrm{A}}}{\sqrt{V_{\mathrm{w}}^2 + v_{\mathrm{A}}^2}}. \tag{3}$$

With the above expression (2), one obtains the mean-squared velocity $\langle v^2(\vartheta) \rangle$ of the bi-spherically distributed pick-up ions by the following expression:

$$\langle v^2(\vartheta) \rangle = \frac{1}{\left[1 - \left(v_{\mathrm{A}} / \sqrt{V_{\mathrm{w}}^2 + v_{\mathrm{A}}^2}\right)\right]} \int_{\cos \vartheta_{\max}}^{1} \left[v_{\mathrm{A}}^2 + (V_{\mathrm{w}}^2 + v_{\mathrm{A}}^2) - 2 v_{\mathrm{A}} \sqrt{V_{\mathrm{w}}^2 + v_{\mathrm{A}}^2} X \right] \mathrm{d}X, \tag{4}$$

which easily reduces to the following expression:

$$\langle v^2(\vartheta)\rangle = V_\mathrm{w}^2\left[1-\frac{v_\mathrm{A}}{\sqrt{V_\mathrm{w}^2+v_\mathrm{A}^2}}\right]+2v_\mathrm{A}^2 \leq V_\mathrm{w}^2. \tag{5}$$

This now permits to account for the fact that the initial energy $\Xi_i = (1/2)m_\mathrm{p}V_\mathrm{w}^2$ of freshly injected secondary ions, after a first violent period of wave-driving, is then reduced to an average energy $\epsilon_i = (1/2)m_\mathrm{p}\langle v^2(\vartheta)\rangle$. This also means, on the other hand, that the energy $\Delta\epsilon_i = \Xi_i - \epsilon_i$ must have been pumped into the ambient turbulent wave field, mainly at or around the injection wavenumber $|k_i| \simeq \Omega_\mathrm{p}/V_\mathrm{w}$. The loss of free energy to the wave fields at the occurence of a redistribution from the initial torus configuration onto the bi-spherical configuration is thereby properly taken into account. Taking into account that $v_\mathrm{A} \ll V_\mathrm{w}$ and equation (5) then manifests that the free energy $\Delta\epsilon_i$ may be represented as

$$\Delta\epsilon_i \simeq \frac{1}{2}m_\mathrm{p}V_\mathrm{w}^2\kappa(1-2\kappa), \tag{6}$$

where $\kappa = v_\mathrm{A}/V_\mathrm{w} \simeq \kappa_0 = \kappa(r_0)$.

It should be noted here that the generation of MHD wave power by newly born energetic ions with subsequent quasi-steady dissipation and plasma heating can of course not only take place in the solar wind plasma regime, but principally in any magnetized partially ionized space plasma with differential bulk velocities of atoms and ions. Such processes may reveal to be important in the interstellar plasma near the boundaries between different interstellar medium (ISM) phases. For example, they can easily result in strongly enhanced high-frequency MHD turbulence powers in the regions downstream of supernova shock fronts propagating through the unprocessed ISM (see section 8).

3. Dissipation of wave power to the plasma ions and associated ion heating

Following previous studies [5–7, 17, 18], we here consider two main heating sources of solar wind protons. The first of these is connected with the background turbulence that is convected radially outwards with the solar wind. The solar wind transports turbulent energy distributed over a wide range of wavenumbers k, showing [19, 20] a so-called 'flicker' spectrum at the smallest wavenumbers up to a critical wavenumber k_0 (*i.e.* energy containing range), and a typical inertial spectrum from the critical wavenumber upwards up to the solar proton dissipation wavenumber $k_\mathrm{dis} \cong \Omega/v_\mathrm{A}$. Here Ω denotes the proton gyrofrequency, and v_A is the Alfven velocity. Existence of the inertial spectral range means that the turbulent energy is cascading down from the turbulence outer scale k_0 to the proton dissipation scale, *i.e.* to the wavenumber $k_\mathrm{dis} = \Omega/v_\mathrm{A}$, and thereby is absorbed in parts by primary and secondary (*i.e.* pick-up) solar wind protons [18]. Convected turbulence thus serves as one of the two relevant heat sources for these two ion species.

The turbulence outer scale k_0 can be defined from the condition that the inverse increment of nonlinear spectral cascading approximately becomes equal to the convection time [5, 6]. In the frame of this model, the rate of energy density dissipation is represented in the following form [5, 6]:

$$\Phi_k(k = k_0, r) = \Phi_0\left(\frac{r}{r_0}\right)^{-s}, \tag{7}$$

with Φ_0 being the corresponding value at the reference heliocentric distance $r = r_0 = 1$ AU given by

$$\Phi_0 = \Phi_k(k = k_0, r_0) = \frac{G_0(V_w B_0^2)}{(4\pi r_0)}, \tag{8}$$

where the factor G_0 is the fractional turbulence level at $r = r_0$, *i.e.*

$$\left\langle \frac{\delta B_0^2}{4\pi} \right\rangle \approx G_0 \rho_0 v_{A0}^2. \tag{9}$$

The power exponent s in equation (9) depends on the low-frequency and on the inertial-range spectral indices. However, in the most interesting case of the low frequency 'flicker' spectrum with a 1D-power exponent $\eta = 1$, the power exponent s has a common value $s = 3$ for both, Kolmogorov (1D spectral index in the inertial range $\lambda = 5/3$) and Kraichnan ($\lambda = 3/2$) turbulence spectra [5, 6].

It should also be mentioned here that Leamon *et al.* [21] using WIND magnetic data argued that the dissipation scale at heliocentric distances of $\sim$1 AU is possibly connected with the value $k_{dis} \simeq \Omega/v_{th}$, where v_{th} is the ion thermal speed. In the outer heliosphere at $r \gg 1$ AU, this scale is of the same order as the inverse inertial scale $k_{dis} = \Omega/v_A$, which leaves the possibility of using one of these scales without detailed consideration of the exact dissipation mechanism.

The second source of plasma heating is connected with the dissipation of those MHD waves generated locally by pick-up ions. Because the injection wavenumber $|k_i| \simeq \Omega/V_w$ is much smaller than the dissipation wavenumber $k_{dis} \simeq \Omega/v_{th}$, one can expect that due to nonlinear wave–wave interactions, *i.e.* diffusion in k-space, the energy input cascades both up and down from k_i roughly at equal parts, like in the case of an oscillator that couples its enforced oscillations to nearby oscillator modes by coupling strengths only dependent on $[k_i^2 - k^2]^{-2}$. Taking this into account, we have the following expression for the corresponding pick-up ion heating source

$$Q_i(r) = \frac{1}{2}\beta_{ex}(r)\Delta\epsilon_i \tag{10}$$

In the above equation, $\beta_{ex}(r)$ denotes the local charge exchange rate of solar wind protons with interstellar H-atoms, as well as describing the local rate of pick-up proton injections, and $\Delta\epsilon_i$ is the average energy injected per particle, which is defined in equation (5). The charge exchange rate $\beta_{ex}(r)$ is given by:

$$\beta_{ex}(r) = n_w(r) n_H(r) \sigma_{ex} V_w, \tag{11}$$

where n_w and n_H are the local proton and H-atom densities, respectively [5], and σ_{ex} the charge exchange cross-section.

4. Consistent set of thermodynamic equations for the solar wind and the wave power propagation

In the following, we first formulate the coupled system of enthalpy flow conservation equations to describe the thermodynamics of the two-fluid solar wind plasma consisting of primary and secondary protons in terms of associated pressures P_1 and P_2. Hereby, we take into account the effects of adiabatic cooling and heating. The heating is due to both the diffusive energy flux $Q_b = Q_{b1,2}$ from the convected turbulence power and that from locally generated turbulent energy, $Q_{i1,2}$, locally pumped into the wavefield by freshly injected secondary ions. For these pressures, we obtain the following two-coupled differential equations:

$$\mathrm{div}\left(\frac{\gamma}{\gamma-1}P_1\overrightarrow{V_{\mathrm{w}}}\right)-(\overrightarrow{V_{\mathrm{w}}}\,\mathrm{grad})P_1=-\frac{3}{2}\xi_1\beta_{\mathrm{ex}}(KT_1)+Q_{b1}(r)+Q_{i1}(r), \tag{12}$$

$$\mathrm{div}\left(\frac{\gamma}{\gamma-1}P_2\overrightarrow{V_{\mathrm{w}}}\right)-(\overrightarrow{V_{\mathrm{w}}}\,\mathrm{grad})P_2=\xi_1\beta_{\mathrm{ex}}(1-\epsilon_f)\frac{1}{2}m_pV_{\mathrm{w}}^2+Q_{b2}(r)+Q_{i2}(r), \tag{13}$$

where the following definitions were used

$$Q_{b1,2}(r)=\xi_{1,2}Q_b \tag{14}$$

and

$$Q_{i1,2}(r)=\frac{1}{2}\xi_{1,2}Q_i. \tag{15}$$

While the first term on the RHS of equation (12) describes the removal of thermal energy from the primary ion fluid due to charge exchange reactions with H-atoms, the first term on the RHS of equation (13) describes the simultaneous input of kinetic energy to the secondary ion fluid due to freshly injected ions. Furthermore, K is the Boltzmann constant and m_{p} the proton mass. The quantities $\xi_{1,2}$ are the relative abundances of primary and secondary ions in the two-fluid solar wind, respectively, defined by:

$$\xi_{1,2}=\frac{n_{1,2}}{n_1+n_2} \tag{16}$$

These abundances can be found with the help of the following continuity equations:

$$\mathrm{div}(n_2\overrightarrow{V_{\mathrm{w}}})=-\mathrm{div}(n_1\overrightarrow{V_{\mathrm{w}}})=\xi_1\beta_{\mathrm{ex}} \tag{17}$$

and are given by [22]:

$$\xi_1=\frac{n_1}{n_1+n_2}=\exp\left[-\int_{r_0}^{r}\sigma_{\mathrm{ex}}n'_{\mathrm{H}}\,\mathrm{d}r'\right] \tag{18}$$

and

$$\xi_2=\frac{n_2}{n_1+n_2}=1-\exp\left[-\int_{r_0}^{r}\sigma_{\mathrm{ex}}n'_{\mathrm{H}}\,\mathrm{d}r'\right] \tag{19}$$

The two above expressions (18) and (19) can be simplified for regions $r\geq r_0\geq 5$ AU with the assumption $n_{\mathrm{H}}\simeq \mathrm{const}\simeq n_{\mathrm{H}\infty}$ and then yield:

$$\xi_1=\exp\left[-\Lambda\left(\frac{r}{r_0}-1\right)\right] \tag{20}$$

and

$$\xi_2=1-\exp\left[-\Lambda\left(\frac{r}{r_0}-1\right)\right], \tag{21}$$

with the denotation $\Lambda=n_{\mathrm{H}\infty}\sigma_{\mathrm{ex}}r_0$.

To describe the propagation of spectral wave power, W_k , in the 1D (quasi-isotropic) limit, we use the following equation [23]:

$$\operatorname{div}\left[\left(\frac{3}{2}\overrightarrow{V_{\mathrm{w}}}+\overrightarrow{v_{\mathrm{A}}}\right)W_k\right]-\frac{1}{2}\overrightarrow{V_{\mathrm{w}}}\operatorname{grad}W_k=\frac{\partial}{\partial k}(\Phi_k)+\beta_{\mathrm{ex}}\Delta\epsilon_i\delta(k-k_i), \qquad (22)$$

where Φ_k is the spectral wave power flux as given by [23, 24]

$$\Phi_k(r)=-D_{kk}\frac{\partial}{\partial k}W_k=-C_{kk}kv_{\mathrm{A}}\left(\frac{4\pi kW_k}{B^2}\right)^{\mu}(kW_k) \qquad (23)$$

Here, D_{kk} is the nonlinear wave–wave diffusion coefficient for isotropic turbulence, $C_{kk}\approx 0.1=\mathrm{const}$, and $\mu=1/2$ (or 1) for the Kolmogorov turbulence (or for the Kraichnan turbulence), respectively. The constancy of Φ_k in the k-space yield the spectrum $W_k\sim k^{-\lambda}$ with $\lambda=5/3$ at $\mu=1/2$ and $\lambda=3/2$ at $\mu=1$. The boundary condition for equation (22) can be written in the form

$$\begin{aligned} &W_k(r_0)\sim k^{-\lambda} \quad \text{at } k>k_0(r_0);\\ &W_k(r_0)\sim k^{-\mu} \quad \text{at } k<k_0(r_0),\quad \mu=1;\\ &\int W_k(r_0)\mathrm{d}k=G_0\rho_0 v_{\mathrm{A0}}^2. \end{aligned} \qquad (24)$$

Within the context of the considered problem, the turbulence wave power may be represented as consisting of two parts, *i.e.* the convected part and the part generated by pick-up ions, and thus it can be represented as

$$W_k=W_k^b+W_k^i,\ W_k^b=W_{k0}^b\left(\frac{k}{k_0}\right)^{-\lambda},\quad W_k^i=\beta_{\mathrm{ex}}\Delta\epsilon_i f(k-k_i), \qquad (25)$$

where the turbulence outer scale k_0 is a decreasing function of heliocentric distane r, and $f(k-k_i)$ is some narrow function of a Gaussian type with the width $\Delta k\ll k_i$ [local wave power input equations (6), (10) and (22) should be assumed to be concentrated near $k=k_i=\Omega/V_{\mathrm{w}}$]. The width and the level of $f(k-k_i)$ should be found from the exact solution of equation (22). The heating sources $Q_{b,i}$ can then be defined as

$$Q_b=\Phi_{k_0},\quad Q_i=\Phi_{k_i+0.5\Delta k}-\Phi_{k_0}. \qquad (26)$$

Equations (12)–(26) consistently describe the quasi-stationary thermodynamics of the solar wind ions coupled to the wave power propagation. Taking into account the discussion presented in section 3 together with the expression (26), the expression for the heating sources can then be simplified to

$$Q_b=\Phi_{k_0},\quad Q_i=\frac{1}{2}\beta_{\mathrm{ex}}\Delta\epsilon_i. \qquad (27)$$

5. Thermodynamics of the solar wind and pick-up protons

We will now make use of the assumption $V_{\mathrm{w}}\simeq V_{\mathrm{w0}}\gg v_{\mathrm{A}}\simeq v_{\mathrm{A0}}$ valid at distances $r\geq 1$ AU. We further assume that the two components of the solar wind plasma can be considered as monoatomic ion gases, suggesting $\gamma_1=\gamma_2=5/3$. Then the equations (12) and

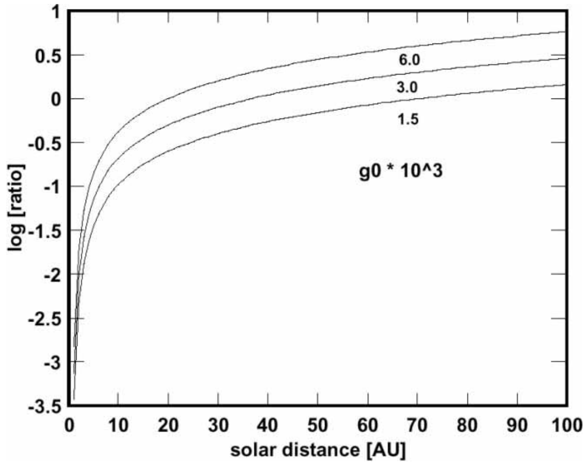

Figure 1. Shown is the ratio $R = Q_{i,1}/Q_{k,1}$ of wave energy absorbed by solar wind protons from pick-up ion driven turbulences and from convected turbulences, respectively, as a function of solar distance in AU. A parametrization is shown for different values of g_0, mainly determined by the LISM neutral H-atom density. The other relevant parameters are adopted with $G_0 = 0.1$ and $s = 9/3$.

(13), when reduced to equations for the temperatures $T_{1,2}$ by setting $P_{1,2} = \xi_{1,2} n_{\rm w} K T_{1,2}$ with $n_{\rm w} = n_{\rm w0}(r_0/r)^2$, allow to find the following equations for T_1 and T_2, respectively [5, 6]

$$\frac{\mathrm{d}}{\mathrm{d}x}T_1 + \frac{4}{3}\frac{T_1}{x} = T_s\left[G_0 x^{2-s} + g_0 \exp\left(-\frac{\Lambda_1}{x}\right)\right] \tag{28}$$

and

$$\frac{\mathrm{d}}{\mathrm{d}x}T_2 + \frac{4}{3}\frac{T_2}{x} + \frac{\beta_{\rm ex} T_2 r_0}{n_2 V_{\rm w}} = \frac{\beta_{\rm ex} m_{\rm p} V_{\rm w} r_0 (1-\epsilon_f)}{3 n_2 K} + T_s\left[G_0 x^{2-s} + g_0 \exp\left(-\frac{\Lambda_1}{x}\right)\right], \tag{29}$$

where we have introduced the following new denotations:

$$x = \frac{r}{r_0}, \quad T_s = \frac{2 m_{\rm p} v_{\rm A}^2}{3K}, \quad \Lambda_1 = \Lambda\left(\frac{V_{\rm w}}{V_{\rm H\infty}}\right)\left(\frac{n_0}{n_{\rm H\infty}}\right),$$

and

$$g_0 = \Lambda\left(\frac{V_{\rm w}}{2v_{\rm A}}\right)\left(\frac{1-2v_{\rm A}}{V_{\rm w}}\right).$$

In the following, we shall discuss the most important results of the above theoretical derivations and, for that purpose, select appropriate values for the relevant parameters appearing in the upper calculations: with [25, 26] $n_{\rm H\infty} = 0.05\,\mathrm{cm}^{-3}$ and $\sigma_{\rm ex}(440\,\mathrm{km/s}) = 2\times 10^{-15}\,\mathrm{cm}^2$ one obtains as a standard value $\Lambda = n_{\rm H\infty}\sigma_{\rm ex} r_0 = 1.5\times 10^{-3}$. With $n_{\rm w0} = 7\,\mathrm{cm}^{-3}$ and $V_{\rm w} = 440\,\mathrm{km/s}$, one then obtains, for example, the critical ionization distance by $\Lambda_1 r_0 = \Lambda(n_{\rm w0}V_{\rm w}/n_{\rm H\infty}V_{\rm H\infty})r_0 = 3.7\,\mathrm{AU}$. The standard value of the parameter $g_0 = \Lambda(V_{\rm w}/4v_{\rm A})$ for these standard values thus amounts to $g_0 = 3.3\times 10^{-3}$ adopting the Alfven speed with $v_{\rm A} = 50\,\mathrm{Km/s}$. As the standard value for $G_{00} = \langle\delta B^2/4\pi\rangle/(\rho_0 v_{\rm A}^2)$, we may take here $G_{00} = 0.1$. Using these above relations and adopting the values $V_{\rm H\infty} = 25\,\mathrm{km/s}$, $s = 9/3$, and $G_{00} = 0.1$, we find the ratio of primary ion heating by pick-up ion-induced – over convected – turbulence power, *i.e.* $R_{i/b} = Q_{i1}/Q_{b1}$, as shown in figure 1 and the temperature profiles $T_1(x, V_{\rm w})$ as shown by figure 2.

As one can see in figure 1, the heating by pick-up ion-induced turbulence, depending on the value for the quantity g_0, *i.e.* for Λ, starts to dominate over heating by convected turbulences from distances of 15 AU outwards to about 50 AU.

Inspection of figure 2 shows that the solar wind ion temperatures T_1 first fall off rapidly with increasing solar distances r. Then in the region between 20 through 30 AU they reach a minimum and beyond they start even to slightly increase with increasing distance. The sensitivity of the temperatures T_1 to the actual solar wind bulk velocities V_{w} thereby is clearly pronounced and recognizable. As we can show by comparing the results of figure 1 with 50-day averages of VOYAGER-2 temperature data [1], our theoretical curves do nicely guide the observed fluctuating temperature values in the ranges 5 through 15 AU and 25 through 40 AU, whereas in the region in between the measured temperature values by some reason seem to be fairly on the low side of theoretical values (see figure 1 in [6]). The T_1-fluctuations are evidently influenced by associated fluctuations in the solar wind bulk velocities V_{w}.

The velocity-dependence of $T_1(x)$ emphasized in the results of figure 2 also becomes especially interesting in view of the fact that, at least under solar minimum conditions, strong systematic variations of the solar wind velocity with latitude have been recognised [27, 28]. This invites us here to study a little more in detail the latitudinal temperature $T_1(\vartheta)$-variation to be expected from this fact. In order to base our study on experimental data, we start again from ULYSSES plasma measurements published in [27], and representing typical solar minimum conditions of the heliosphere. As obtained from the first full polar orbit passage of ULYSSES, the essential solar wind parameters scaled to a reference distance of $r_0 = 1$ AU, such as bulk velocity $V_{\mathrm{w}0}$, density $n_{\mathrm{w}0}$, and proton temperature $T_{1,0}$, have been obtained as functions of solar latitude angle ϑ.

In figure 3, we have shown the temperatures $T_1(r, \vartheta)$ obtained as a function of solar distance for different solar latitudes ϑ. As can be seen there, within latitudes $0° \le \vartheta \le 20°$ temperatures are nearly insensitive to latitude and distance. However, then with increasing latitudes $30° \le \vartheta \le 60°$, there appears a fairly strong latitude dependence. As a hint for a better understanding of the data, it is perhaps important to recognise that the latitudinal gradient in T_1 is much more pronounced than the radial gradient, at least during solar minimum conditions.

In figure 4, we have shown the temperature $T_2 = T_2(x)$ calculated as a function of the solar distance $x \ge x_{20} = 5$ AU along the upwind axis for different parameter values of V_{w}. As it can be seen in figure 4, the temperatures T_2 at all distances are clearly related to the

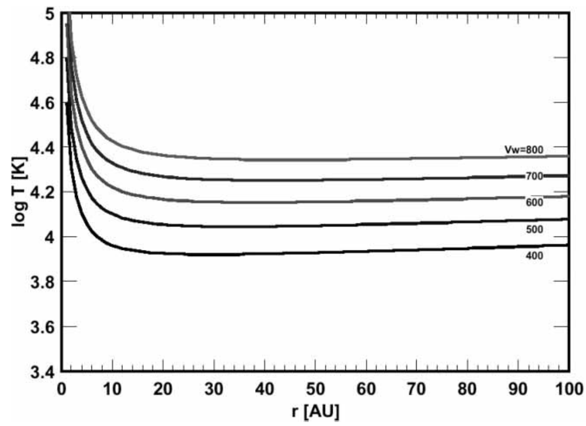

Figure 2. Shown as a function of the solar distance in upwind direction is the solar wind proton temperature T_1 for various solar wind bulk speeds V_{w}. Solar wind density, Alfven speed, and the values of g_0 and G_0 have been changed in accordance with V_{w}.

solar wind bulk velocity, and, at larger solar distances, behave with distance fairly isothermal as was already pointed out earlier in papers by Fahr [29]. In view of the latitudinal solar wind velocity gradient that is evident at solar activity minimum conditions, analogous to the results shown in figure 3, we can thus, in view of figure 4, also expect that strong latitudinal gradients in the temperatures T_2 to be present. The secondary ion fluid definitely will show higher temperatures T_2 at higher heliographic latitudes. Figure 4 clearly shows that the secondary ion temperatures $T_2(x)$ have a pronounced sensitivity to the solar wind bulk speeds V_w, since initial and asymptotic values are pure functions of V_w, with the change-over in the profiles being determined by other competing parameters such as the values for g_0, G_0, v_A, and s.

6. Kinetic views: kinetic ion transport and spectral power transport

In this part of the paper, we consider some kinetic aspects of the particle physics in the outer heliosphere. The proton distribution function resulting in the interface as a consequence of charge-exchange induced exchanges between the distributions of protons and H-atoms suggests [9, 10] that this distribution function f_p in first order may represent a superposition of two shifted Maxwellians with different partial densities n_0 and n_1 and different bulk velocities U_1 and U_2. We briefly discuss here the wave-particle relaxation of the disturbed distribution functions in the heliospheric interface. For this purpose, we need to define typical characteristics of MHD turbulence in the interface downstream of the outer LISM bow shock. We assume that the interface turbulence originates from the interaction of MHD waves convected inwards by the local interstellar plasma flow with the bow shock at the outer border of the interface. Considering the transformation of MHD turbulence at the bow shock have shown that [11], independent of the bow shock geometry, the turbulence in the postshock interface region clearly appears to be dominated by incompressible Alfven waves (the ratio between incompressible and compressible fluctuations increases by about one order of magnitude at the bow shock), and furthermore that waves propagating towards the shock are more intensive than those escaping from there.

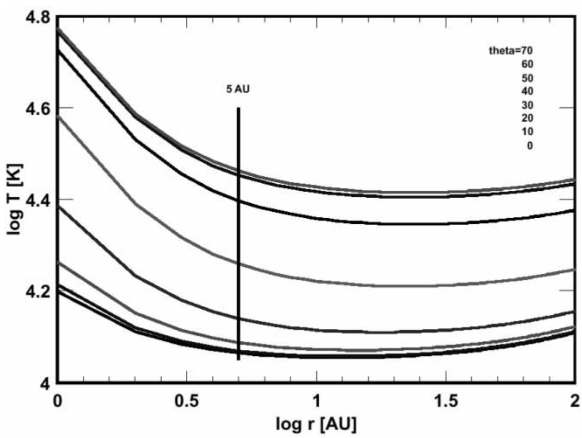

Figure 3. Shown as a function of solar distance is the solar wind proton temperature T_1 for various heliographic latitudes. Consistent with the change in latitude also the solar wind bulk speed and density, the Alfven speed, and the parameters g_0 and G_0 have been changed. The initial boundary values for T_1 at 5 AU have been taken from [28].

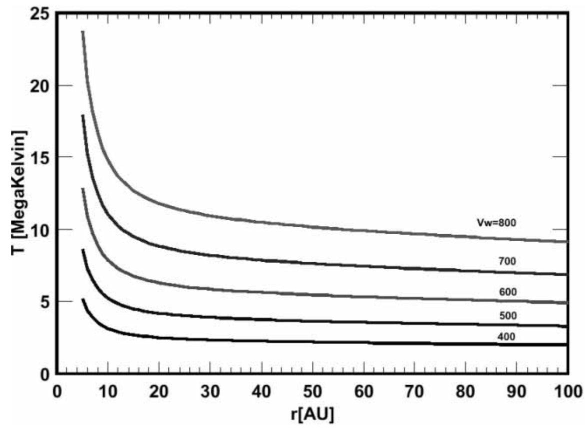

Figure 4. Shown as a function of solar distance in upwind direction is the pick-up ion temperature T_2 in units of megakelvin for various solar wind speeds V_w. All relevant input parameters have been changed in accordance with the change in V_w.

In accordance with the above conclusion, we consider the relaxation of newly produced H/O-ions created by charge exchange of protons with H/O-atoms due to their interactions with the turbulence in the interface. Quasilinear interactions of H/O-ions with Alfven turbulence are possible at the resonance conditions

$$\pm k_{\parallel} v_a - k_{\parallel} \mu v = n \Omega_{\mathrm{H,O}}, \tag{30}$$

where n can attain the values $n = 0, \pm 1, \pm 2, \ldots$, $k_{\parallel}$ is the component of the wave vector $\overrightarrow{k}$ parallel to the magnetic field, v the individual ion speed, and μ its pitch-angle cosine. The resonance conditions (30) cannot be fulfilled at $n = 0$, since in our case, $v \leq v_a$ and $\mu \lesssim 1$. As the only possible solution of equation (30) with $k_{\parallel} v_a \leq \Omega_{\mathrm{H,O}}$, one can thus identify the case: $n = -1$, *i.e.* leading to:

$$k_{\parallel} = k_{\mathrm{res,H,O}} = \frac{\Omega_{\mathrm{H,O}}}{\mu v + v_a}, \tag{31}$$

which corresponds to ion resonances with Alfven waves propagating in opposite direction to the bulk of the H/O-atoms.

The quasilinear diffusion coefficient D_{ql}^a describing diffusion in velocity-space can be easily estimated in the model for slab turbulence, *i.e.* assuming only wave propagation along the magnetic field, and is found [30] in the form:

$$D_{\mathrm{ql}}^a \simeq \frac{\pi}{2}(1 - \mu_0^2)\Omega_{\mathrm{H,O}} v_a^2 \frac{|k W_k^-|_{k=k_{\mathrm{res}}}}{B_0^2}, \tag{32}$$

where W_k^- is the 1D spectral power density of the downstream propagating Alfven waves and μ_0 is some typical value of the pitch-angle cosine. One can see from equation (32) that the quasilinear diffusion coefficient is defined by the fractional turbulence level at the wavenumber $k = k_{\mathrm{res}}$.

Now we consider the relaxation of newly created H-ions due to the nonlinear scattering process [31]: $a + p \to a' + p'$, with the energy conservation law

$$k_{1\parallel} v_a - \mathbf{k}_1 \mathbf{v}_1 = k_{2\parallel} v_a - \mathbf{k}_2 \mathbf{v}_2. \tag{33}$$

As it follows from the above relation, the particle velocity and pitch angle changes are comparatively small, *i.e.*:

$$\Delta\mu \simeq \frac{\Delta v}{v} \simeq \frac{v_a}{v} \leq 1. \tag{34}$$

Consequently, the processes of pitch-angle scattering and velocity magnitude change are of a diffusion type with nearly equal diffusion rates in both coordinates. The diffusion coefficient D^a can then be estimated [31] by:

$$D^a_{\mathrm{nl}} \simeq \frac{v_a^2 T_{\mathrm{H}}^2}{(T_{\mathrm{H}} + T_{\mathrm{e}})^2} \frac{4\pi \int \omega W^a_\omega \,\mathrm{d}\omega}{B_0^2}, \tag{35}$$

where $T_{\mathrm{H,e}}$ are the temperatures of newly created protons and electrons of the local interface plasma and W^a_ω the temporal power spectrum of the Alfven turbulence.

The comparison between equation (32) for D^a_{ql} and equation (35) for D^a_{nl} shows that these coefficients only differ by a numerical factor of the order of unity. The characteristic diffusion time τ^a_{bg} thus can be estimated as

$$\tau^a_{\mathrm{bg}} \simeq \frac{(U_{\mathrm{H}} - U_{\mathrm{p}})^2}{D^a_{\mathrm{ql}} + D^a_{\mathrm{nl}}}. \tag{36}$$

Using the recent data on the turbulence in LISM and the wave transformation coefficients at the bow shock (36), the following numerical estimate of the wave-particle relaxation time (36) can be found [11]

$$\tau^a_{\mathrm{bg}} = \tau^{\mathrm{wp}}_{\mathrm{rel}} \simeq 10^8 \text{ s}. \tag{37}$$

The above estimate shows that relaxation due to the interaction with the background Alfven turbulence appears to be a fairly slow process for plausible interface parameters, *i.e.* comparatively low turbulence levels. However, the time $\tau^{\mathrm{wp}}_{\mathrm{rel}}$ given above is comparable with the particle transport time τ_{tr} through the interface, *i.e.*: $\tau_{\mathrm{tr}} \simeq 5 \times 10^8$ s. This may clearly indicate that the resulting distribution functions in the outer interface region can be expected to reveal non-equilibrium signatures. This is especially true for the O-ions for which relaxation processes run much slower and corresponding relaxation periods are even longer yielding $\tau^a_{\mathrm{bg,O}} \simeq \sqrt{16}\tau^a_{\mathrm{bg}} \simeq 4 \times 10^9$ s.

7. Kinetic aspects of ISM turbulence generation by supernova shockwaves

The most promiment structures in interstellar space are supernova (SN) shock fronts. At the position of running SN shock, the interstellar plasma has to pass from the upstream to the downstream side of this shock. This passage has a strong influence on the ion distribution function and leads to the generation of squeezed, strongly anisotropic functions with free, non-relaxated energy that can drive turbulences. Due to mechanisms already mentioned, this free energy is at least partly pumped into fluctuation powers of low-frequency MHD turbulences. Here we shall try to shortly estimate the resulting effects for the average ISM MHD turbulence.

To describe the evolution in time and space of MHD turbulence originating at SN shockwaves, one needs to look at the evolution of the SN shock dynamics at the propagation of

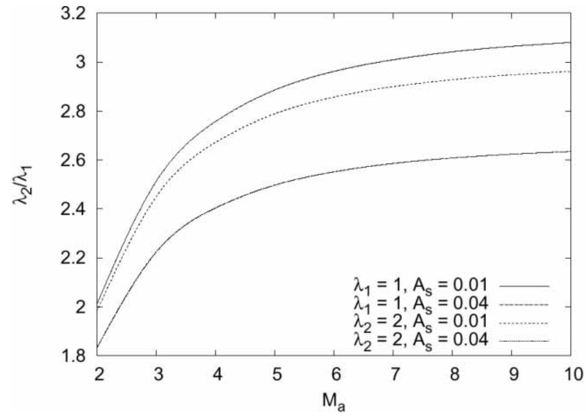

Figure 5. Shown is the ratio of the downstream to the upstream ion pressure anisotropy λ_2/λ_1 at the (perpendicular) SN shock as a function of the upstream Machnumber M_a, for different combinations of upstream values for the pressure anisotropy λ_1 and the upstream plasma beta A_s.

the shock through the interstellar space. Relying on the Sedov solution for the SN blast wave evolution at its protrusion into the ambient ISM, one can describe the SN propagation velocity $U_1 = U_1(t)$ as a function of time by the following relation [32, 33]

$$U_1(t) = \frac{2}{5}\left(\frac{2E_{\mathrm{SN}}}{\rho_1}\right)^{1/5} t^{-3/5}, \tag{38}$$

where E_{SN} denotes the total energy released by the SN explosion and ρ_1 is the ambient interstellar gas mass density ahead of the propagating shock.

One may keep in mind that the compression ratio s, as given by the Rankine–Hugoniot relations, is expressed as:

$$s(t) = \frac{(\gamma+1)M_1^2(t)}{(\gamma-1)M_1^2(t)+2} \tag{39}$$

and is time-dependent via $M_1(t)$, *i.e.* the upstream Mach number of the plasma flow. This number depends on SN shock evolution time t and can be given by:

$$M_1^2(t) = \frac{\rho_1 U_1^2(t)}{\gamma P_1} = \frac{4}{25}\frac{\rho_1^{3/5}}{P_1}(2E_{\mathrm{SN}})^{2/5} t^{-6/5}. \tag{40}$$

Realising now that the propagating SN shock essentially acts as a perpendicular MHD shock, one can then solve the following Boltzmann–Vlasow equation [12] written in coordinates of the comoving plasma bulk frame and describing the change of the ion population at the passage of the ISM plasma along the shock normal coordinate 's' when passing from the upstream to the downstream side of the shock front

$$\frac{\mathrm{d}}{\mathrm{d}s}\bar{f}(w_\parallel, w_\perp, s) = \left\{\left(\frac{w_\perp}{2B}\frac{\mathrm{d}B}{\mathrm{d}s}\right)\frac{\mathrm{d}}{\mathrm{d}w_\perp}\right\}\bar{f}(w_\parallel, w_\perp, s). \tag{41}$$

Here $\bar{f}(w_\parallel, w_\perp, s)$ is the ion distribution function in the plasma bulk frame written as a function of the space coordinate s and of the velocity coordinates $w_\parallel$ and $w_\perp$, parallel and perpendicular to the local magnetic field B, respectively. The above differential equation can be solved starting from the upstream distribution function $\bar{f}_1(w_\parallel, w_\perp)$ and delivering the downstream distribution function $\bar{f}_2(w_\parallel, w_\perp)$. From this distribution function, the downstream pressure anisotropy can be obtained as a ratio of the following two moments of $\bar{f}_2(w_\parallel, w_\perp)$ by

$$A_2 = \frac{P_{\perp 2}}{P_{\parallel 2}} = \frac{\int d^3 w w_\perp^2 \bar{f}_2(w_\parallel, w_\perp)}{\int d^3 w w_\parallel^2 \bar{f}_2(w_\parallel, w_\perp)}. \tag{42}$$

In figure 5, we show how the resulting downstream ion pressure anisotropy behaves as a function of the upstream Mach number M_1, or the compression ratio σ, of the SN shock. From this figure, one can see that starting from an isotropic upstream distribution function one ends up at the downstream side of an SN shock with Mach numbers $M_1 \geq 6$ with a highly anisotropic ion distribution of an anisotropy of $A_2 \geq 2.6$.

The resulting downstream distribution functions $\bar{f}_2(w_\parallel, w_\perp)$ may be unstable with respect to the so-called mirror-mode instability [34], which has its onset if

$$\frac{\beta_\perp}{\beta_\parallel} \geq \frac{1+\beta_\perp}{\beta_\perp}, \tag{43}$$

where the usual definition of the plasma beta-values has been used, *i.e.*

$$\beta_{\perp,\parallel} = \frac{P_{\perp,\parallel}}{(B^2/8\pi)}. \tag{44}$$

The mirror-mode instability drives low-frequency ($\omega \ll \Omega_g = eB/mc$) magneto-acoustic waves with $|\vec{k}| = k_\perp$, and the energy ϵ_{turb} per unit volume, which in total can be transferred to the following turbulences downstream of the shock:

$$\epsilon_{\text{turb}} \simeq (P_{2\perp} - \tilde{P}_{2\perp}), \tag{45}$$

where $P_{2\perp}$ and $\tilde{P}_{2\perp}$ are the corresponding downstream pressures resulting immediately after shock passage and after a mirror-mode driven relaxation to the marginally mirror-mode stable pressure, respectively. The latter quantity can be calculated assuming that during the relaxation process, $P_{2\parallel}$ is not changed to amount to

$$\frac{\tilde{P}_{2\perp}}{P_{2\parallel}} = \frac{B^2}{8\pi} \frac{1 + (\tilde{P}_{2\perp}/(B^2/8\pi))}{\tilde{P}_{2\perp}}, \tag{46}$$

which yields the marginally stable pressure,

$$\tilde{P}_{2\perp} = P_{2\parallel} + \sqrt{\frac{P_{2\parallel}^2}{4} + \frac{B^2 P_{2\parallel}}{8\pi}}. \tag{47}$$

From the above result, one can derive

$$\epsilon_{\text{turb}} \simeq \left(P_{2\perp} - P_{2\parallel} - \sqrt{\frac{P_{2\parallel}^2}{4} + \frac{B^2 P_{2\parallel}}{8\pi}} \right), \tag{48}$$

which furthermore leads to

$$\epsilon_{\text{turb}} \simeq P_{2\perp} \left(1 - \frac{1}{A_2} \left(1 + \sqrt{\frac{1}{4} + \frac{1}{\beta_{2\parallel}}} \right) \right). \tag{49}$$

For weakly magnetized plasmas, *i.e.* high β-values, with $A_2 \simeq 2.6$, one then derives

$$\epsilon_{\text{turb}} \simeq P_{2\perp}\left(1 - \frac{3}{2A_2}\right) = P_{2\perp}\left(1 - \frac{3}{5.2}\right) = 0.43P_{2\perp}. \tag{50}$$

This shows that $\sim 40\%$ of the shock-entropized upstream kinetic ion energy may be converted into downstream magneto-acoustic turbulences, which definitely may also increase the intensity of radio scintillations in the region downstream of an SN shock wave. Judged on a statistical basis, the state of the average ISM getting an imprint from SN shock wave passages from time to time may mean that the levels of magneto-acoustic turbulences due to the wave-driving effect of SN fronts may turn out to be higher than expected up to now.

8. Conclusions

We have shown that energetic ions, appearing in plasmas due to injection of new ions into the magnetized background plasma, flow with their convertible free energy drive turbulences of Alfvenic and magneto-acoustic types. Especially, under the conditions of strongly charge-exchanging fluids with supersonic differential bulk velocities, as occuring in the inner heliosphere, this led to strongly enhanced fluctuation levels. Both the low and high-energy ion populations then also partly reabsorbed these wave energies, and thereby experienced non-thermal heatings. As a quantitative example, we treated the non-adiabatic behaviours of solar wind ions and pick-up ions expanding with the solar wind towards large solar distances. While pick-up ions behaved nearly isothermal, normal solar wind ions even behaved pseudo-polytropically with negative effective polytropic indices describing a temperature increase at the expansion to larger volumes. As we furthermore demonstrated the charge-exchanging plasmas in the inner and outer heliosheath, such as the solar wind and the interstellar ion and atom fluids, led to unexpectedly enhanced turbulence amplitudes of low-frequency Alfven and magneto-acoustic waves. As a consequence of that, lower periods for the relaxation of non-equilibrium ion distribution functions and lower coefficients for the spatial diffusion of galactic cosmic rays could be expected in the heliosheath.

Finally, we studied the interstellar turbulence generation at SN shock fronts due to the generation of mirror-unstable anisotropic distribution ion functions downstream of the shock. As demonstrated, an unexpectedly high percentage of the shock-entropized thermal energy of the downstream ions was converted into magneto-acoustic turbulences, which not only classified the region immediately downstream of the SN shock as a high-turbulence region, but, in a statistical view, also indicated an unexpected increase in the average turbulence levels in the ISM in general.

Acknowledgements

We very much appreciate the financial support through the DFG grant 436 RUS 113/110/12-3, and the Program 'Plasma processes in the solar system' of Russian Academy of Sciences. H.J.F. is also grateful to the financial support granted by the DFG in the frame of the project Fa-97/31-1.

References

[1] P.R. Gazis, A. Barnes, J.D. Mihalov *et al.*, J. Geophys. Res. **99** 6561 (1994).
[2] J.D. Richardson, K.I. Paularena, A.J. Lazarus *et al.*, Geophys. Res. Lett. **22** 325 (1995).

[3] G. Gloeckler, in *SOLAR WIND TEN: Proceedings of the Tenth International Solar Wind Conference*, AIP Conference Proceedings, volume 679 (2003), p. 583.
[4] L.A. Fisk and G. Gloeckler, Astrophys. J. **640** L79 (2006).
[5] H.J. Fahr and I.V. Chashei, Astron. Astrophys. **395** 991 (2002).
[6] I.V. Chashei, H.J. Fahr and G. Lay, Ann. Geophys. **21** 1405 (2003).
[7] S.V. Chalov, D.B. Alexashov and H.J. Fahr, Astron. Lett. **32** 206 (2006).
[8] H.J. Fahr, Adv. Space Res. **34** 3 (2004).
[9] H.J. Fahr and M. Bzowski, Astron. Astrophys. **424** 263 (2004).
[10] H.J. Fahr and M. Bzowski, in *Physics of the Outer Heliosphere*, AIP Conference Proceedings, volume 719, edited by V. Florinski, N.V. Pogorelov and G.P. Zank (Melville, NY., 2004), p. 373.
[11] I.V. Chashei, H.J. Fahr and G. Lay, Solar Phys. **226** 163 (2005).
[12] H.J. Fahr and M. Siewert, Astron. Astrophys. **458** 13 (2006).
[13] C.S. Wu and R.C. Davidson, J. Geophys. Res. **77** 5399 (1972).
[14] A.A. Galeev, A.N. Poludov, R.Z. Sagdeev *et al.*, Sov. Phys. JETP (Engl. Transl.) **65** 1178 (1987).
[15] H.P. Freund and C.S. Wu, J. Geophys. Res. **93** 14277 (1988).
[16] D.E. Huddleston and A.D. Johnstone, J. Geophys. Res. **97** 12217 (1992).
[17] G.P. Zank, W.H. Matthaeus and C.W. Smith, J. Geophys. Res. **101** 17093 (1996).
[18] C.W. Smith, W.H. Matthaeus, G.P. Zank *et al.*, J. Geophys. Res. **106** 8253 (2001).
[19] K.U. Denskat and F.M. Neubauer, J. Geophys. Res. **87** 2215 (1982).
[20] T.S. Horbury and A.J. Balogh, J. Geophys. Res. **106** 15929 (2001).
[21] R.J. Leamon, C.W. Smith, N.F. Ness *et al.*, J. Geophys. Res. **104** 4775 (1998).
[22] H.J. Fahr and D. Rucinski, Space Sci. Rev. **407** 97 (2001).
[23] C.Y. Tu and E. Marsch, Space Sci. Rev. **73** 1 (1995).
[24] Y. Zhou and W.H. Matthaeus, J. Geophys. Res. **95** 14881 (1990).
[25] V.V. Izmodenov, Astrophys. Space Sci. **274** 55 (2000).
[26] H.J. Fahr, Astrophys. Space Sci. **274** 35 (2000).
[27] D.J. McComas, B.L. Barraclough, H.O. Funsten *et al.*, J. Geophys. Res. **105** 10419 (2000).
[28] D.J. McComas, H.A. Elliott, J.T. Gosling *et al.*, Geophys. Res. Lett. **29** 4 (2002).
[29] H.J. Fahr, Solar Phys. **208** 335 (2002).
[30] R. Schlickeiser, Astrophys. J. **336** 243 (1989).
[31] V.N. Tsytovich, *Theory of Turbulent Plasma* (Consultant Bureau, New York, 1977), p. 535.
[32] G.F. Krymski, Akademia Nauk SSSR, Doklady **234** 1306 (1977).
[33] G.F. Krymski, Akademia Nauk SSSR, Doklady **234** 1309 (1977).
[34] R.A. Treumann and W. Baumjohann, in *Advanced Space Plasma Physics* (Imperial College Press, 1997), p. 56.